RSC Advances

PAPER

View Article Online
View Journal | View Issue

Cite this: *RSC Adv.*, 2021, **11**, 6449

The green synthesis of a palm empty fruit bunch-derived sulfonated carbon acid catalyst and its performance for cassava peel starch hydrolysis

Iryanti Fatyasari Nata, *[a] Chairul Irawan, [a] Meilana Dharma Putra [a] and Cheng-Kang Lee[b]

A sulfonated carbon acid catalyst (C–SO_3H) was successfully generated from palm empty fruit bunch (PEFB) carbon *via* hydrothermal sulfonation *via* the addition of hydroxyethylsulfonic acid and citric acid. The C–SO_3H catalyst was identified as containing 1.75 mmol g^{-1} of acid and 40.2% sulphur. The surface morphology of C–SO_3H shows pores on its surface and the crystalline index (CrI) of PEFB was decreased to 63.8% due to the change structure as it became carbon. The surface area of the carbon was increased significantly from 11.5 to 239.65 m^2 g^{-1} after sulfonation *via* hydrothermal treatment. The identification of –SO_3H, COOH and –OH functional groups was achieved using Fourier-transform infrared spectroscopy. The optimal catalytic activity of C–SO_3H was achieved *via* hydrolysis reaction with a yield of 60.4% of total reducing sugar (TRS) using concentrations of 5% (w/v) of both C–SO_3H and cassava peel starch at 100 °C for 1 h. The stability of C–SO_3H shows good performance over five repeated uses, making it a good potential candidate as a green and sulfonated solid acid catalyst for use in a wide range of applications.

Received 2nd January 2021
Accepted 23rd January 2021

DOI: 10.1039/d1ra00019e

rsc.li/rsc-advances

Introduction

In recent years, the interest in the bioconversion of lignocellulosic waste materials to chemicals and fuels has been steadily increasing because of their abundance, low cost, and sustainability.[1,2] One of the most highly produced vegetable oils worldwide is crude palm oil, with 6.93.107 tons produced in 2017.[3] Palm Empty Fruit Bunches (PEFB) are one of the main waste products obtained from the oil palm industry and a main cause of pollution. Concerns about environmental protection have increased over the years from a global point of view. The oil palm industry generates large amounts of solid waste, *i.e.*, PEFB, which is utilized as mulch for preventing erosion and maintaining soil moisture, fertilizer and compost. However, PEFB has little commercial value and is even a disposable problem due to its low bulk density and it thus needing a large storage volume. PEFB is usually used as a fuel in the factory, in which every ton of palm fruit bunch (PFB) processed in the mills consists of 23% of PEFB, 12% of mesocarp fiber, and 5% of shell.[4]

PEFB consists of potential components such as 44.4% of cellulose, 30.9% of hemicelluloses, and 14.2% of lignin, which could be utilized for more useful products.[5,6] Due to the high content of lignocellulosic materials, many researchers have investigated the utilization of PEFB in biodiesel,[7] biogas,[8] ethanol, nanocomposites[9] and other value-added products.[6,10,11] However, there is an increasing need to utilize PEFB at low cost.

Many researchers have tried to produce low-cost activated carbon as an adsorbent using oil palm shell,[12] palm fiber[13] and other carbon.[14] The surface functionalization of carbon can be achieved *via* a hydrothermal method by modifying the carbon surface through a one-step reaction.[11,15] In addition, no research has been found to utilize PEFB in terms of their conversion to a solid acid catalyst. Solid acid catalysts are a type of catalyst that can be economically and ecologically applied in catalysis. These catalysts have many advantages compared to common liquid acid catalysts, such as fewer disposal problems, they are non-corrosive, reusable, environmentally benign and easy to handle. Recently, incomplete carbonization of sugars during the preparation of sulfonated carbon was reported, in which the process resulted in better catalytic activity in the synthesis of biodiesel compared with other solid acid catalysts, including sulfonated zirconia, Nafion, and niobic acid.[16] Catalytic reactions based on solid acid catalysts using reactants such as glycerol,[17] cellulose,[18] hemicelluloses[19] and starch[20] have been confirmed as effective. However, the acid content of the catalyst depends on the carbon structure used as a template for modification. In order to increase the catalyst performance, surface functionalization on carbon structure can be achieved due to porous structure of PEFB.

Based on our knowledge, no research has been reported on the synthesis of sulfonated carbon solid acid catalysts from PEFB as a carbon source *via* hydrothermal treatment. Herein,

[a]*Department of Chemical Engineering, Lambung Mangkurat University, Banjarbaru 70714, Indonesia. E-mail: ifnata@ulm.ac.id*

[b]*Department of Chemical Engineering, National Taiwan University of Science and Technology, Taipei 106, Taiwan*

a green process of producing a sulfonated carbon acid catalyst (C–SO_3H) from PEFB was conducted. The carbon formation and sulfonation process were expected to produce a high acid content, with sulfonate and carboxyl groups on the catalyst. In this work, the effect of the sulfonation process on the structure of the carbon was evaluated. The physical properties of the original material, carbon, and C–SO_3H, such as their surface morphology, crystalline structure, surface functional groups, and surface area were characterized. C–SO_3H was applied in cassava peel starch hydrolysis. Furthermore, the utilization of cassava peel starch as a substrate is also one strategy for making value-added products from food waste. The reusability of C–SO_3H was also investigated to evaluate the catalyst performance. The results of this research could be useful in the field of catalysis and also relevant to the environment, especially in the utilization of waste biomass.

Experimental methods

Chemicals

PEFB and cassava peel were collected from PT. Pola Kahuripan Inti Sawit, Kintapura, South Kalimantan, Indonesia and a traditional local market, respectively. D-Glucose ($C_6H_{12}O_6$), citric acid ($C_6H_5Na_3O_7 \cdot 2H_2O$), 3,5-dinitrosalicylic acid ($C_7H_4N_2O_7$), hydroxyethylsulfonic acid ($C_2H_6O_4S$), phenolphthalein ($C_{20}H_{14}O_4$), sodium hydroxide (NaOH), methanol (CH_3OH), sodium chloride (NaCl), chloride acid (HCl), sulfuric acid (H_2SO_4) and oxalic acid ($H_2C_2O_4$) were purchased from Sigma-Aldrich.

Preparation of the sulfonated carbon solid acid catalyst

The PEFB was washed with tap water and then dried in an oven at 100 °C, then ground into a powder using a high speed blender to gain a material with a size that passes through a 60 mesh sieve. The PEFB (500 g) was heated in a furnace (muffle furnace, Hema scientific instruments) at 350 °C for 30 min under an inert atmosphere.[21] The obtained carbon (C) was sulfonated *via* a hydrothermal treatment according to procedure reported in the literature,[22] with slight modification. Briefly, 1.5 g of citric acid, 2.5 g of hydroxyethylsulfonic acid and 30 g of carbon were added to 40 mL of deionized (DI) water, and this solution was then placed in a Teflon-lined stainless steel autoclave (50 mL). The reaction was then carried out at 180 °C for 4 h in an oven. The carbon material was obtained after filtration and sequential washing of the reaction product using DI water, methanol and then DI water. The C–SO_3H product was then dried in an oven at 80 °C overnight.

Preparation of the cassava peel starch and hydrolysis reaction

Cassava peel (2 × 2 cm) was blended in the presence of DI water, with a cassava peel ratio of 1 : 4. After filtration, the precipitate was dried for 24 h at 90 °C in an oven and then sieved to pass through a 40 mesh. The hydrolysis of the cassava peel starch (2.5%; 5.0%; 7.5%; 10%, w v^{-1}) was conducted in a three-necked glass flask reactor (100 mL) in a close system with the addition of C–SO_3H (2.5%; 5.0%; 7.5%; 10%, w v^{-1}) and DI water (50 mL) at 100 °C for 60 min. The hydrolysed product was obtained *via* centrifugation and analysis of an aliquot of the solution was conducted using the 3,5-dinitrosalicylic acid (DNS) method to measure the total reducing sugar (TRS).[23] To examine the catalyst performance, concentrated sulfuric acid as a common homogeneous catalyst and the carbon from the PEFB as a general heterogeneous catalyst were also tested in the hydrolysis reaction. All data are presented as averages of experimental results that were carried out in triplicate.

C–SO_3H was treated to allow for its repeated use. The recovered C–SO_3H was rinsed three times by stirring in DI water for 45 min and then collected when the filtrate was ~pH 7. After separation from the liquid, it was then dried at 80 °C overnight in an oven.

Characterization

A neutralization titration method was used to calculate the Brønsted acid sites on C and C–SO_3H.[24] Briefly, the carbon materials (80 mg) and a solution of 1 M NaCl (40 mL) were mixed with stirring for 6 h at room temperature. After centrifugation, the supernatants were obtained and then titrated using 0.01 N NaOH with phenolphthalein as an indicator. X-ray fluorescence (XRF) measurements were used to detect elements in the samples using a PANalytical/Minipal machine. The surface areas of the materials were calculated *via* Brunauer–Emmett–Teller (BET) characterization using a nitrogen adsorption–desorption type Quantachrome Autosorb-1 instrument. Scanning Electron Microscope (SEM) measurements were carried out using a JEOL JSM-6500 LV microscope to analyze the surface morphologies of the samples. A Rigaku D/MAX-B X-ray diffractometer equipped with a copper K-alpha (Cu Kα) radiation source was used in the X-ray diffraction (XRD) measurements at a voltage of 40 kV and current of 100 mA. Fourier-transform infrared spectroscopy (FT-IR, Bio-rad, Digilab FTS-3500) was utilized to analyze the functional groups on the carbon surface in the wavelength range of 4000–400 cm^{-1} at a scan rate of 8. Thermogravimetric analysis (TGA) was conducted to identify the weight loss of the samples using a platinum crucible over the temperature range of 30 to 600 °C under a flow of nitrogen at a specific heating rate of 10 °C min^{-1} (PerkinElmer, Diamond TG/DTA). The carbon content of the particles and degradation of the components were calculated from the weight loss percentages of the TGA curves. The TRS was analyzed using the DNS method[23] and analyzed by UV-vis spectroscopy with a V-550-JASCO spectrometer.

Results and discussion

Characterization of the sulfonated solid acid catalyst

The formation of the C–SO_3H catalyst was conducted *via* a two-step reaction. First, PEFB fiber was carbonized to produce carbon. The second step involved the sulfonation of the carbon *via* hydrothermal treatment. All of the preparation steps of the generation of C–SO_3H from PEFB are presented in Fig. 1.

Materials changes of the surface morphology of PEFB were observed by SEM (Fig. 2), where from the SEM images it can be seen that the original structure of the PEFB fibers was fibrous with a smooth surface. The PEFB consists of cellulose, hemicelluloses and lignin that still bind to each other (Fig. 2a). The

Fig. 1 Preparation steps of the generation of C–SO_3H from PEFB.

PEFB is pyrolyzed, dehydrated –C–O–C-dissociation occurs and then the final step is polycyclic aromatic carbon ring formation at 350 °C to form the carbon structure.[25,26] After carbonization, the surface structure of the PEFB is coarse and porous. This is possibly due to the heating process during carbonization causing the cellulose, hemicelluloses and lignin compounds to break down into three main components of carbon, tar and gas (volatile matter) (Fig. 2b). The sulfonation process *via* the hydrothermal treatment leads to the surface of the carbon becoming more porous (Fig. 2c). Hydroxyethylsulfonic and citric acids were added to the hydrothermal treatment as coupling agents to functionalize the carbon with sulfonate and carboxylic groups, respectively.

A hydrothermal (HT) system is a spontaneous and exothermic reaction, the majority product of this system is carbon. The operating temperatures of HTC widely found over 100 °C in nature because many minerals are formed under these conditions. Materials are formed under vacuum *via* hydrothermal conditions have increased solubility, which facilitates the physical and chemical interactions between reagents and solvent and also ionic and acidic reactions.[27] The HT process enhances the acidity level of the C–SO_3H by up to 7.3-fold compared to the level of C. Compared to C, the surface area of C–SO_3H is also significantly increased from 11.5 to 239.65 m^2 g^{-1}. Upon going from C to C–SO_3H, the pore volume increased from 0.018 to 0.137 cm^3 g^{-1}. The nitrogen adsorption–desorption isotherms for C and C–SO_3H are illustrated in Fig. 3. The carbon material exhibits a type IV isotherm with a H3-type hysteresis loop, which indicates the mesoporous structure of C–SO_3H. Besides this, C–SO_3H is more stable and water-tolerant to hydrothermal conditions than other solid acid catalysts.[24]

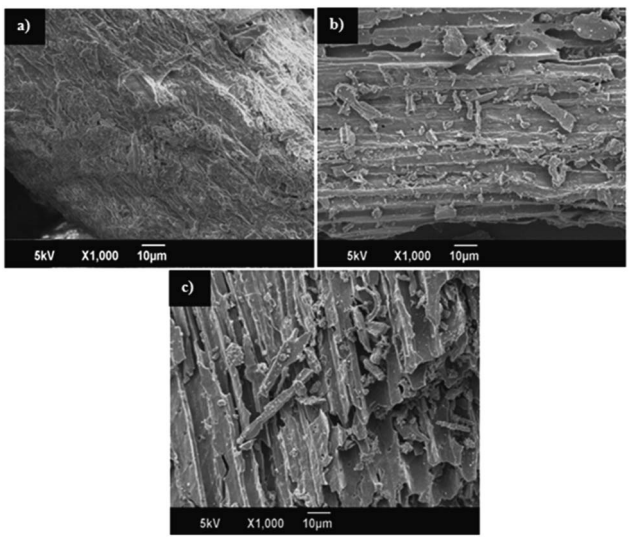

Fig. 2 SEM images of (a) PEFB, (b) PEFB after carbonization and (c) the sulfonated carbon solid acid catalyst (C–SO_3H).

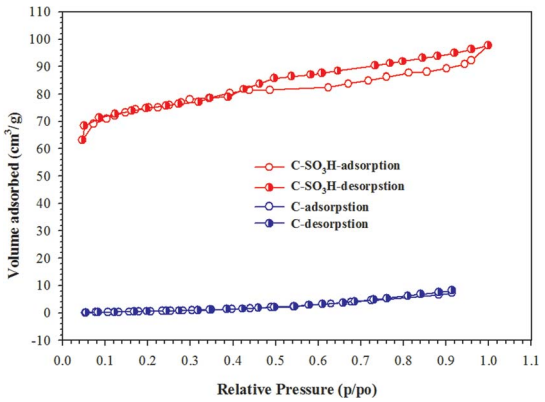

Fig. 3 The nitrogen adsorption–desorption isotherm of PEFB after carbonization (C) and the sulfonated carbon solid acid catalyst (C–SO_3H).

The sulfonic acid groups were formed on the catalyst through the reaction of a sulfonating agent with the aromatic rings of the carbon *via* electrophilic substitution.[28,29] It was reported that the surface functionalization of the polycyclic aromatic carbon rings with sulfonate groups generates a large number of thermally stable acid sites, and furthermore, leads to the stacking of sulfonate groups at the edges of the carbon rings.[30] XRF analysis shows the sulphur content on the carbon to be around 40.2%, which indicates that sulfonation of the carbon was achieved to form an amorphous structure, with this type of structure being composed of polycyclic aromatic carbon sheets with sulfonate and carboxylic groups. The detailed results of the characterization of PEFB, C, and C–SO_3H are presented in Table 1.

The crystalline index (CrI) is a measure of the regularity of the crystal structure of a material. The breaking of the structure of PEFB led to a decrease in its crystalline index of 63.8% (Fig. 4). The XRD pattern shows the changes in the intensity of an amorphous area at $2\theta = 17°$ and cellulose crystals at $2\theta = 22.8°$.[31] The decrease in the CrI values occurs because the crystallinity of the structure is lost as the material is converted into carbon during carbonization. Only high intensity of the cellulose crystal area was observed for PEFB. Similar results for the carbon and sulfonated solid acid catalysts were observed, indicating that no structural changes occurred during the sulfonation treatment.

After the sulfonation process, the appearance of bands at 1207 and 1720 cm^{-1} was recorded due to sulfonate group (Fig. 5); with the presence of sulfonate groups also confirmed elsewhere in the literature.[32] The band observed at 3400 cm^{-1} can be attributed to the –OH in carboxylic acid groups; which indicates that the sulfonation process not only creates sulfonate groups but also forms other functional groups because of

Table 1 The characterization of the PEFB fiber, C, and C–SO_3H

Sample	Sulphur content (%)	Acidity (mmol g^{-1})	Surface area (m^2 g^{-1})	Pore volume (cm^3 g^{-1})
PEFB fiber	—	—	0.171	—
C	—	0.21	11.55	0.018
C–SO_3H	40.2	1.75	239.65	0.137

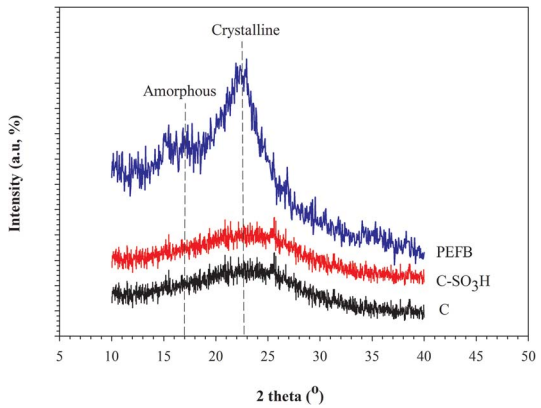

Fig. 4 XRD patterns of PEFB, C and C–SO_3H.

oxidization reactions.[33] Polyaromatic C=C bond peaks were observed at 1608 cm^{-1}, which signed as a carbon material.

TGA was conducted to study the type of thermal degradation of the material and impact of sulfonation on C–SO_3H. Fig. 6 shows the TGA of the materials carbonized up to 600 °C. The dehydration of the water of the PEFB sample began at 74.4 °C, continued upon the decomposition of cellulose and hemicellulose in the range of 240–320 °C, and the next degradation in this was that of lignin at 320–380 °C. For both materials, the reduction in mass was due to the decomposition of carbon and the thermal process also enhanced their oxidized structure, thus reducing their thermal stability.[25] The TGA curves also show that the mass loss trend of C–SO_3H is around 8% more than that of C. At temperatures in the range of 140–240 °C, the

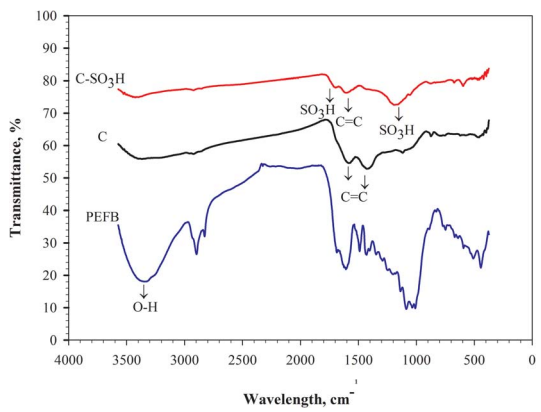

Fig. 5 FT-IR spectra of PEFB, C and C–SO_3H.

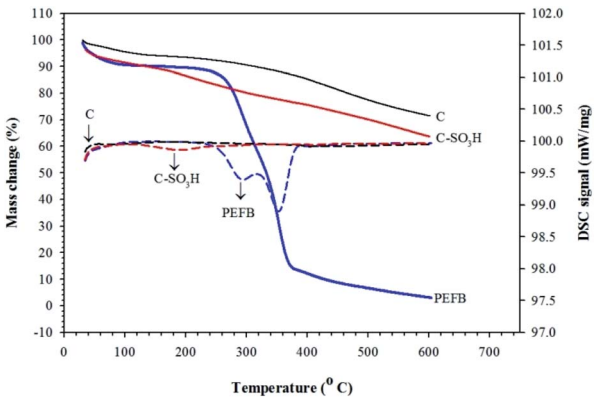

Fig. 6 TGA analysis curves of PEFB, C, and C–SO_3H.

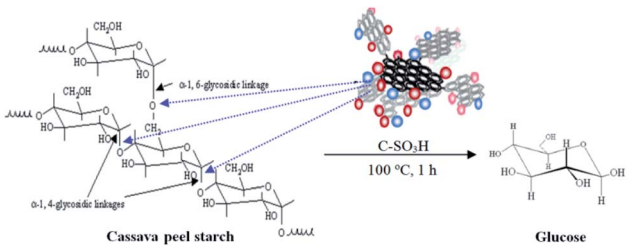

Fig. 7 Schematic diagram of the hydrolysis of cassava peel starch by C–SO_3H.

material is rapidly degradated in the case of C–SO_3H, possibly related to the number of sulfonate groups present on the carbon. As reported, C–SO_3H sulfonated by sulfonate groups has a weak structure and is unstable compared to the original carbon.[21]

Hydrolysis of cassava peel starch over the sulfonated carbon solid acid catalyst

One of the potential raw materials for glucose production is carbohydrate, as it can be converted into glucose *via* a hydrolysis reaction using a heterogeneous/homogeneous catalyst and

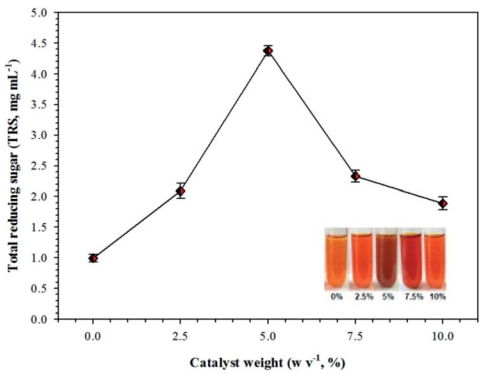

Fig. 8 Total reducing sugar (TRS) of cassava peel starch hydrolysis in terms of the variation in the weight of the C–SO_3H catalyst. Reaction conditions: 5% (w v^{-1}) of cassava peel starch, 100 °C, 1 h.

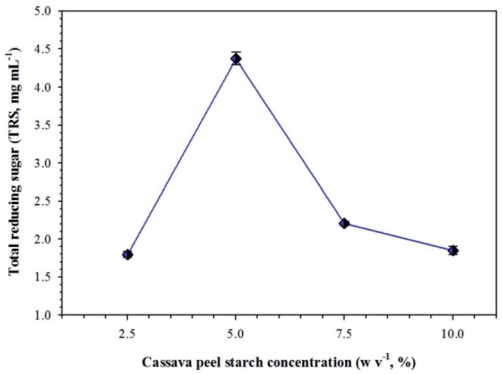

Fig. 9 Total reducing sugar (TRS) of the cassava peel starch hydrolysis in terms of the variation in cassava peel starch concentration. Reaction condition: 5% (w v^{-1}) C–SO_3H, 100 °C, 1 h.

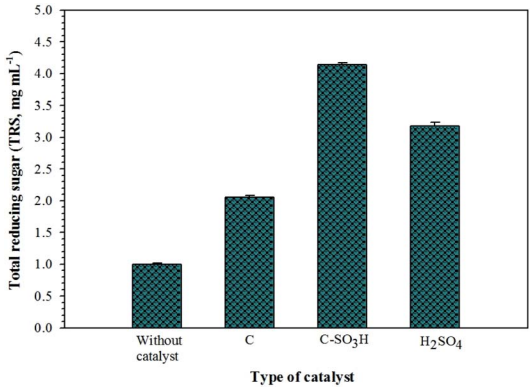

Fig. 10 Total reducing sugar (TRS) of cassava peel starch hydrolysis over different types of catalysts. Reaction condition: 5% (w v^{-1}) of cassava peel starch and C–SO_3H, 100 °C, 1 h.

an enzymatic reaction. The cassava peel starch used in this research consists of 80.2% carbohydrate. The C–SO_3H breaks the α-(1,6)-and α-(1,4)-glycosidic bonds in the starch chain to produce an oligomer of glucose. The schematic diagram of the hydrolysis of cassava peel starch by C–SO_3H is shown in Fig. 7.

The hydrolysis performance with a variation of catalyst concentration is presented in Fig. 8. The TRS as a hydrolysis product was increased when the weight of C–SO_3H was increased up to 5%, with a TRS produced of 4.375 mg mL^{-1}. The presence of C–SO_3H as a catalyst in cassava peel starch hydrolysis significantly increased the amount of product produced by around 4.4-fold compared to hydrolysis without a catalyst. This

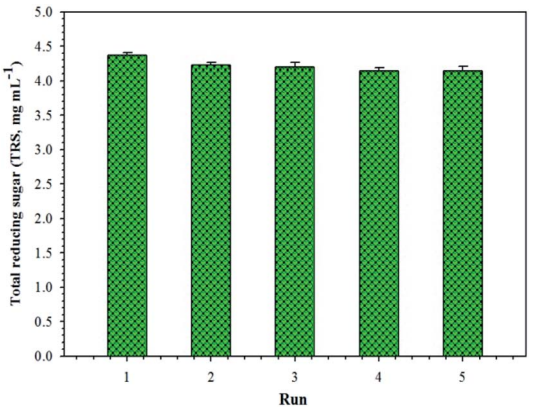

Fig. 11 Catalytic performance of C–SO_3H during its fifth repeated use in cassava peel starch hydrolysis. Reaction conditions: 5% (w v^{-1}) of cassava peel starch and C–SO_3H, 100 °C, 1 h.

means that the catalytic performance of C–SO_3H increases due to it being modified *via* surface functionalization. The concentration of TRS regularly decreased at higher C–SO_3H concentration (>5%) because the formed sugar compounds degraded into furfural.[34] Its also becomes a key point in hydrolysis in terms of high temperature and prolonged time.[35] The hydrolysis performance of C–SO_3H was also observed to show TRS compared with sulfonated catalysts that use corn on the cob as a carbon precursor.[36]

The TRS produced was indicated by color intensity, and the DNS assay was used to evaluate this intensity. The color of the solution obtained was more orange and a higher color intensity showed the presence of a higher concentration of TRS (Fig. 8, inset).

The high TRS concentration was obtained because the catalyst has access and can easily attach to the carbohydrate linkage. Furthermore, the concentration of the cassava peel starch as a substrate is at its optimal at 5% in terms of producing TRS (Fig. 9). A higher concentration of starch leads to a more viscous solution due to the swelling and gelatinization of starch in the presence of water. Thus, these conditions make it more difficult for C–SO_3H to access the carbohydrate linkage, hence resulting in a lower TRS. Based on the energy efficiency and consumption costs of the hydrolysis reaction, a concentration of 5% cassava peel starch using 5% C–SO_3H was selected as the optimal conditions.

In order to determine the reactivity of C–SO_3H, it is interesting to investigate the performance of C and H_2SO_4 as

Table 2 The catalytic activity of sulfonated acid catalysts in hydrolysis

Catalyst	Acidity (mmol g^{-1})	Solvent	Method	Temp (K)/time (h)	TRS yield (%)	Ref.
30-CCSA	0.86	H_2O	HT	423/6	44.52	37
PCPs–SO_3H	1.80	H_2O	—	393/3	5.30	38
CM–SO_3H	4.22	[BMIM][Cl]	—	303/3	59.4	39
CSA–SO_3H	1.76	H_2O	Microwave	403/1	34.6	40
C–SO_3H	1.75	H_2O	—	373/1	64.0	This work

heterogeneous and homogeneous catalysts, respectively. C was used as a control, whereas the H^+ ion concentration of H_2SO_4 used was the same concentration as the H^+ ion content of C–SO_3H. As shown in Fig. 10, TRS values of around 2.05 and 3.18 mg mL^{-1} were obtained using C and H_2SO_4 as catalysts, respectively. The reaction using the C–SO_3H catalyst has a higher TRS value of around 1.02-fold than that using C. However, the common liquid catalyst (H_2SO_4) showed lower performance (TRS value of 3.18 mg mL^{-1}) compared to C–SO_3H. This is probably due to the presence of –SO_3H and –COOH groups that functionalize the carbon. Furthermore, H_2SO_4 only has H^+ ions in the homogenous phase and it should be easy for the catalyst to access and attach to a carbohydrate linkage.

Table 2 shows that the sulfonated carbon acid catalyst prepared in this work is more efficient and has higher hydrolysis activity than other sulfonated solid catalysts, even those prepared using difficult methods in ionic liquids or water using HT and microwave methods. In order to investigate the activity of the catalyst for repeated uses, the recovered C–SO_3H was used in another cycle of hydrolysis. The recovered catalyst performance was observed to be slightly lower than that achieved in the 1st reaction. The decrease in TRS was observed to be only 5.3% after five repeated uses until the TRS result was fairly constant (Fig. 11). The decrease in activity is due to the loss of active sites from catalyst during washing, decreasing the acidity of C–SO_3H to around 5.14%. In addition, the sulfonated carbon solid catalyst is easy to handle and almost 98% was recovered. This proves that C–SO_3H provides effective hydrolysis of starch into glucose. This result also shows that the prepared C–SO_3H not only is a non-toxic material, prepared *via* a green process and is easy to handle, but also shows good catalytic performance for hydrolysis reactions.

Conclusions

Carbon with a high acid content, rich in sulfonate and carboxyl groups, was prepared from PEFB by sulfonation *via* a hydrothermal treatment. Hydroxyethylsulfonic and citric acids were used as sources for the sulfonate and carbonyl groups, respectively. Good performance and stability of the sulfonated acid catalyst in cassava peel starch hydrolysis were shown after five repeated uses. Simple operation, high catalytic activity and utilization of waste materials are the important advantages in the development of this sulfonated solid acid catalyst. The synthesized catalyst has great potential to be developed for use in green process and also various catalyst applications.

Conflicts of interest

There are no conflicts to declare.

Acknowledgements

The authors wish to thank the Directorate General of Research and Community Services, Ministry of Research, Technology and Higher Education, Republic of Indonesia, who provided the research grant (contract No. 122.9/UN8.2/PL/2019).

References

1 Z. Sun, G. Bottari, A. Afanasenko, M. C. A. Stuart, P. J. Deuss, B. Fridrich and K. Barta, *Nat. Catal.*, 2018, **1**, 82–92.
2 S. Sae-ngae, B. Cheirsilp, Y. Louhasakul, T. T. Suksaroj and P. Intharapat, *Sustainable Environ. Res.*, 2020, **30**, 11.
3 E. A. Ocampo Batlle, Y. Castillo Santiago, O. J. Venturini, J. C. Escobar Palacio, E. E. Silva Lora, D. M. Yepes Maya and A. R. Albis Arrieta, *J. Cleaner Prod.*, 2020, **250**, 119544.
4 G. Najafpour, H. A. Yieng, H. Younesi and A. Zinatizadeh, *Process Biochem.*, 2005, **40**, 2879–2884.
5 F. Fahma, S. Iwamoto, N. Hori, T. Iwata and A. Takemura, *Cellulose*, 2010, **17**, 977–985.
6 U. U. Ndubuisi-Nnaji, U. A. Ofon, N. I. Ekponne and N.-A. O. Offiong, *Sustainable Environ. Res.*, 2020, **30**, 14.
7 Z. Yaakob, I. S. B. Sukarman, B. Narayanan, S. R. S. Abdullah and M. Ismail, *Bioresour. Technol.*, 2012, **104**, 695–700.
8 S. O-Thong, K. Boe and I. Angelidaki, *Appl. Energy*, 2012, **93**, 648–654.
9 N. Saba, M. T. Paridah, K. Abdan and N. A. Ibrahim, *Mater. Chem. Phys.*, 2016, **184**, 64–71.
10 S. K. Loh, S. James, M. Ngatiman, K. Y. Cheong, Y. M. Choo and W. S. Lim, *Ind. Crops Prod.*, 2013, **49**, 775–781.
11 G. K. Parshetti, S. Kent Hoekman and R. Balasubramanian, *Bioresour. Technol.*, 2013, **135**, 683–689.
12 K. Y. Foo and B. H. Hameed, *Desalination*, 2011, **275**, 302–305.
13 B. H. Hameed, I. A. W. Tan and A. L. Ahmad, *J. Hazard. Mater.*, 2008, **158**, 324–332.
14 X.-H. Zhang, Q.-Q. Tang, D. Yang, W.-M. Hua, Y.-H. Yue, B.-D. Wang, X.-H. Zhang and J.-H. Hu, *Mater. Chem. Phys.*, 2011, **126**, 310–313.
15 F. Merzari, M. Lucian, M. Volpe, G. Andreottola and L. Fiori, *Chem. Eng. Trans.*, 2018, **65**, 43–48.
16 H. Xiao, Y. Guo, X. Liang and C. Qi, *J. Solid State Chem.*, 2010, **183**, 1721–1725.
17 W. Han, X. Li, S. Yu and X. Sang, *Chem. Eng. Trans.*, 2018, **65**, 547–552.
18 O. L. Li, R. Ikura and T. Ishizaki, *Green Chem.*, 2017, **19**, 4774–4777.
19 P. L. Dhepe and R. Sahu, *Green Chem.*, 2010, **12**, 2153–2156.
20 D. Yamaguchi and M. Hara, *Solid State Sci.*, 2010, **12**, 1018–1023.
21 Y. N. Ma'rifah, I. F. Nata, H. Wijayanti, A. Mirwan, C. Irawan, M. D. Putra and H. Kawakita, *Int. J. Technol*, 2019, **10**, 512–520.
22 H. Xiao, Y. Guo, X. Liang and C. Qi, *J. Solid State Chem.*, 2010, **183**, 1721–1725.
23 G. Miller, *Anal. Chem.*, 1959, **31**, 426–428.
24 A. Onda, T. Ochi and K. Yanagisawa, *Green Chem.*, 2008, **10**, 1033–1037.
25 J. R. Kastner, J. Miller, D. P. Geller, J. Locklin, L. H. Keith and T. Johnson, *Catal. Today*, 2012, **190**, 122–132.
26 A. d. C. Fraga, C. P. B. Quitete, V. L. Ximenes, E. F. Sousa-Aguiar, I. M. Fonseca and A. M. B. Rego, *J. Mol. Catal. A: Chem.*, 2016, **422**, 248–257.

27 B. Hu, K. Wang, L. Wu, S.-H. Yu, M. Antonietti and M.-M. Titirici, *Adv. Mater.*, 2010, **22**, 813–828.
28 A. Aldana-Pérez, L. Lartundo-Rojas, R. Gómez and M. E. Niño-Gómez, *Fuel*, 2012, **100**, 128–138.
29 I. M. Lokman, M. Goto, U. Rashid and Y. H. Taufiq-Yap, *Chem. Eng. J.*, 2016, **284**, 872–878.
30 M. Okamura, A. Takagaki, M. Toda, J. N. Kondo, K. Domen, T. Tatsumi, M. Hara and S. Hayashi, *Chem. Mater.*, 2006, **18**, 3039–3045.
31 H. Zhao, J. H. Kwak, Z. Conrad Zhang, H. M. Brown, B. W. Arey and J. E. Holladay, *Carbohydr. Polym.*, 2007, **68**, 235–241.
32 R. Ormsby, J. R. Kastner and J. Miller, *Catal. Today*, 2012, **190**, 89–97.
33 E. M. Santos, A. P. d. C. Teixeira, F. G. da Silva, T. E. Cibaka, M. H. Araújo, W. X. C. Oliveira, F. Medeiros, A. N. Brasil, L. S. de Oliveira and R. M. Lago, *Fuel*, 2015, **150**, 408–414.
34 E. Palmqvist and B. Hahn-Hägerdal, *Bioresour. Technol.*, 2000, **74**, 25–33.
35 I. F. Nata, C. Irawan, P. Mardina and C.-K. Lee, *J. Solid State Chem.*, 2015, **230**, 163–168.
36 I. F. Nata, M. D. Putra, D. Nurandini and C. Irawan, *Int. J. Adv. Sci. Eng. Inf. Technol.*, 2017, **7**, 1302–1308.
37 S. Shen, B. Cai, C. Wang, H. Li, G. Dai and H. Qin, *Appl. Catal., A*, 2014, **473**, 70–74.
38 H. Guo, Y. Lian, L. Yan, X. Qi and R. L. Smith, *Green Chem.*, 2013, **15**, 2167–2174.
39 X. Qi, Y. Lian, L. Yan and R. L. Smith, *Catal. Commun.*, 2014, **57**, 50–54.
40 Y. Jiang, X. Li, X. Wang, L. Meng, H. Wang, G. Peng, X. Wang and X. Mu, *Green Chem.*, 2012, **14**, 2162–2167.